On gravity currents in stratified ambients

V. K. Birman and E. Meiburg[a)]
Department of Mechanical Engineering, University of California, Santa Barbara, California 93106, USA

M. Ungarish
Department of Computer Science, Technion, Haifa 32000, Israel

(Received 29 December 2006; accepted 3 May 2007; published online 8 August 2007)

Detailed numerical simulations were conducted of gravity currents released from a lock and propagating at the bottom of a linearly stratified ambient. The objective is to test the predictions of the recent theoretical analysis by Ungarish [M. Ungarish, J. Fluid Mech. **548**, 49 (2006)] concerning the dependency of the front velocity (Froude number, Fr) on the stratification parameter (S) and height ratio (a). The functional dependence of the front velocity on S is found to agree with the theoretical results for weak stratification, although the numerically obtained front velocities lie below the predicted values, as a result of viscous effects. Simulations for deeply submerged currents (small a) in strongly stratified ambients ($S>0.5$) show that the front velocities deviate from the fastest predicted theoretical solution, but fall within the range of the slower solutions found by Ungarish. This observation supports the theoretical prediction concerning (a) the existence of multiple solutions; and (b) the selection of the slowest solution as the front velocity in a nonforced time-dependent flow. The computational results point to the action of internal waves as the cause for the reduced front velocity. The numerical results also confirm the prediction that the thickness ratio of current to ambient is less than one half, and decreases with S. © *2007 American Institute of Physics*. [DOI: 10.1063/1.2756553]

I. INTRODUCTION

Gravity currents represent a ubiquitous phenomenon in nature and technical applications, as demonstrated by the many examples provided in the book by Simpson.[1] Following the seminal work by Benjamin,[2] they have motivated a large number of experimental, theoretical, and, more recently, computational investigations into their properties under a wide variety of conditions. In the current context, the propagation of gravity currents into stratified ambients is of particular interest. Several investigations have addressed such flows in the past. Experimental studies[3–5] focus on the generation of internal waves by continuous release gravity currents. On the other hand, Maxworthy *et al.*[6] perform both experiments and numerical simulations of lock release currents, in order to study the effect of internal waves on the motion of the gravity current.

Very recently, Ungarish[7] extended Benjamin's classical analysis to the propagation of a gravity current into a stratified ambient. Toward this end, he adopted Long's solution for Boussinesq stratified flow over topography[8–10] to obtain the description of the velocity and density fields behind the gravity current front. Ungarish was able to derive an equation for the front velocity of the gravity current as a function of the stratification and front height. This equation can be solved analytically in the limit of small stratification parameters. The results are close to Benjamin's prediction for a similar depth ratio, but slightly reduced by the stratification. However, for a stronger stratification and small front heights a significant departure from the classical behavior is predicted. A striking feature is that multiple stable solutions exist, and it is not clear which one will be attained in a real flow. (We recall that Ungarish's and Benjamin's solutions are for steady state flows.) Ungarish argues that for a gravity current starting from rest in the multiple solutions regime the front attains the slowest solution first, and then keeps moving with that velocity. Since the theoretical analysis is based on a number of simplifying assumptions, the predictions obtained from it have to be tested, which constitutes the goal of the present investigation. Toward this end, we will conduct highly resolved, two-dimensional simulations that provide detailed information about the temporal and spatial evolution of the velocity and density fields. Note that we limit this investigation to lock release currents.

In Sec. II we provide the fundamental equations governing the flow and define the nondimensional parameters. Detailed numerical results are obtained in Sec. III, and compared with the theoretical predictions by Ref. 7. Concluding remarks are provided in Sec. IV.

II. FLOW CONFIGURATION AND GOVERNING EQUATIONS

Figure 1 shows the configuration employed in the two-dimensional simulations to be discussed in the following. A lock of length L_c and height H_c is embedded in a rectangular channel of length L and height H. Simulations with $H_c=H$ are referred to as full lock release, while for $H_c<H$ we have a partial lock release. The ratio of lock height to channel height is referred to as fractional depth, $h_c=H_c/H$.

a)Author to whom correspondence should be addressed. Electronic mail: meiburg@engineering.ucsb.edu

 © 2007 American Institute of Physics

Downloaded 13 Jan 2009 to 130.95.144.214. Redistribution subject to AIP license or copyright; see http://pof.aip.org/pof/copyright.jsp

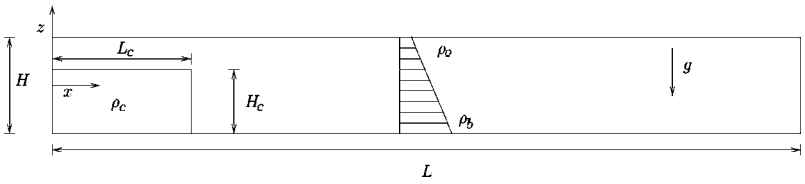

FIG. 1. A lock of length L_c and height H_c releases fluid of density ρ_c into a channel of length L and height H. Initially, the ambient fluid has a linear density stratification ranging from ρ_b at the bottom wall to ρ_o at the top.

Initially the lock is filled with fluid of density ρ_c, while the ambient fluid exhibits a linear density stratification ranging from ρ_b at the bottom to ρ_o at the top of the channel. Since $\rho_c \geq \rho_b$, a gravity current forms along the bottom surface once the gate is opened at $t=0$. In following our earlier work,[11,12] we employ the incompressible Navier-Stokes equations for variable density flows in the form,

$$\nabla \cdot \mathbf{u} = 0, \tag{1}$$

$$\rho \frac{D\mathbf{u}}{Dt} = \rho \mathbf{g} - \nabla p + \nabla \cdot (2\mu \mathbf{S}), \tag{2}$$

$$\frac{D\rho}{Dt} = K\nabla^2 \rho, \tag{3}$$

where g represents the gravitational acceleration, p indicates pressure, μ refers to the dynamic viscosity, and $\mathbf{S}$ denotes the rate of strain tensor. The molecular diffusivity is indicated by K. Note that we do not invoke the Boussinesq approximation. Based on scaling arguments discussed in Ref. 12, we neglect diffusive effects in the continuity equation.

In order to nondimensionalize the above set of equations, the lock height H_c is taken as the length scale, while the density ρ_c of the lock fluid serves as the characteristic density. Velocities are scaled by the buoyancy velocity $u_b = \sqrt{g(1-r_o)H_c}$, where $r_o = \rho_o/\rho_c$. Since the current velocity will be of the same order as the buoyancy velocity, the current can thus be expected to propagate about one lock height per dimensionless time unit. We arrive at the following set of governing dimensionless equations:

$$\nabla \cdot \mathbf{u} = 0, \tag{4}$$

$$\rho \frac{D\mathbf{u}}{Dt} = \frac{1}{1-r_o}\rho \mathbf{e_g} - \nabla p + \frac{1}{\mathrm{Re}} \nabla \cdot (2\rho \mathbf{S}), \tag{5}$$

$$\frac{D\rho}{Dt} = \frac{1}{\mathrm{Pe}}\nabla^2 \rho. \tag{6}$$

Only horizontal channels are considered, so that e_g is given by the unit vector $(0,-1)$. Three governing dimensionless parameters appear in Eqs. (4)–(6), viz. the density ratio r_o, the Reynolds number $\mathrm{Re} = u_b H_c/\nu$, and the Péclet number $\mathrm{Pe} = u_b H_c/K$. Based on the observation that the Schmidt number $\mathrm{Sc} = \mathrm{Pe}/\mathrm{Re}$ influences the results only weakly, we employ $\mathrm{Pe} = \mathrm{Re}$ in all simulations.

Following Ref. 7, we measure the magnitude of the stratification by introducing

$$S = \frac{\rho_b - \rho_o}{\rho_c - \rho_o} = \frac{r_b - r_o}{1 - r_o}, \tag{7}$$

where $r_b = \rho_b/\rho_c$. We keep r_o fixed at 0.9 in all simulations, and vary S by modifying r_b.

In discussing the simulation results, the front velocity U_{gc} will play a pivotal role. As will be seen, there are two meaningful ways to render U_{gc} dimensionless. In order to be consistent with the theoretical analysis of Ungarish,[7] we define a dimensionless front velocity U_H based on the lock height H_c, and a Froude number Fr_h based on the front height h, according to

$$U_H = \frac{U_{gc}}{\sqrt{g(1-r_o)H_c}}, \tag{8}$$

$$\mathrm{Fr}_h = \frac{U_{gc}}{\sqrt{g(1/r_o - 1)h}}. \tag{9}$$

Equations (4)–(6) are solved in the vorticity-stream-function formulation, employing the computational approach described in Birman *et al.*[11] Slip conditions are enforced along all of the walls, in order to facilitate the comparison with the

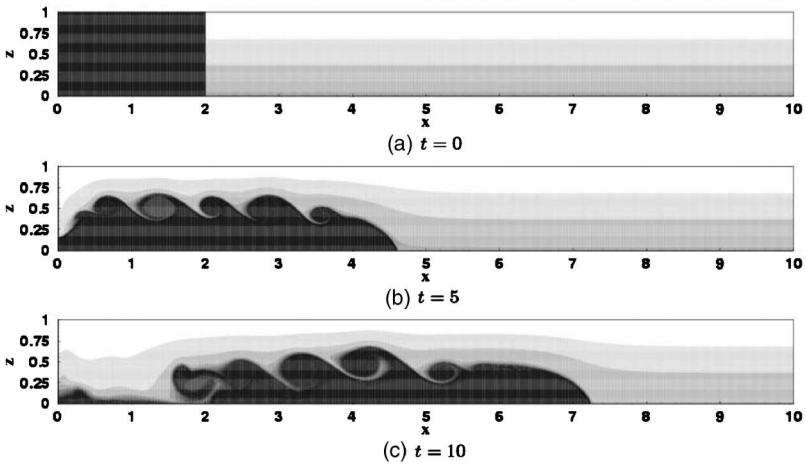

FIG. 2. Gravity current for a stratification parameter value of $S=0.2$ and an initial fractional depth $h_c=1$. The concentration contours show the formation of an advancing front, behind which a vigorous Kelvin-Helmholtz instability gives rise to strong vortices.

Downloaded 13 Jan 2009 to 130.95.144.214. Redistribution subject to AIP license or copyright; see http://pof.aip.org/pof/copyright.jsp

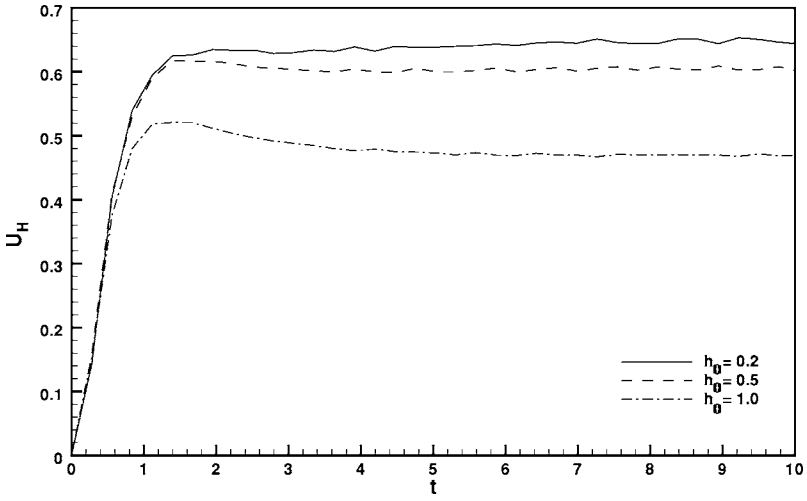

FIG. 3. Propagation velocity U_H as a function of time for gravity currents with S=0.2, Re=4000 and h_c=1, 0.5, and 0.2, respectively. After the initial adjustment phase, each front moves with a nearly constant velocity.

inviscid theoretical treatment by Ungarish,[7] while Neumann boundary conditions are imposed on the concentration field.

In the following, we limit ourselves to two-dimensional simulations, although from experiments and simulations we know that gravity currents give rise to three-dimensional features. Even though the lobe-and-cleft structures and spanwise instabilities of the dominant Kelvin-Helmholtz vortices cannot be captured by the two-dimensional simulations, these effects are well known to have little effect on the height and propagation velocity of the flow, which are the main quantities of interest here.[13]

III. RESULTS

In this section, we discuss observations from several numerical simulations, and provide comparisons with some of the key results of Ungarish.[7]

A. Representative simulations

We discuss three representative cases of gravity current flows in stratified ambients. All of them correspond to a stratification of S=0.2 and Re=4000, while the fractional depth h_c is set to 1, 0.5, and 0.2, respectively. In each case, the gravity current undergoes a short initial adjustment phase and moves with constant velocity thereafter for several lock lengths (the slumping phase). The propagation velocity and front height of the gravity current represent the primary quantities of interest. The propagation velocity is evaluated as the velocity with which the $\rho=0.5(1+r_b)$ contour advances along the wall. The value $0.5(1+r_b)$ represents the average density of the lock fluid and the ambient fluid at the bottom wall, so that it is suitable for tracking the front. The distance of this contour above the wall provides the local height $h_l(x)$ of the gravity current. We will give a brief physical description of the flows, before comparing their main features with the theoretical predictions of Ref. 7.

1. Full lock release

Figure 2 shows the concentration contours of the flow with an initial fractional depth h_c=1. After the adjustment phase the gravity current moves with a nearly constant velocity, as seen in Fig. 3. Note that the head is not raised, due to the slip condition applied at the lower wall. The concentration contours do not indicate the presence of significant internal waves that might affect the gravity current.[6] The mixing layer behind the current head is characterized by a Kelvin-Helmholtz instability that results in the generation of

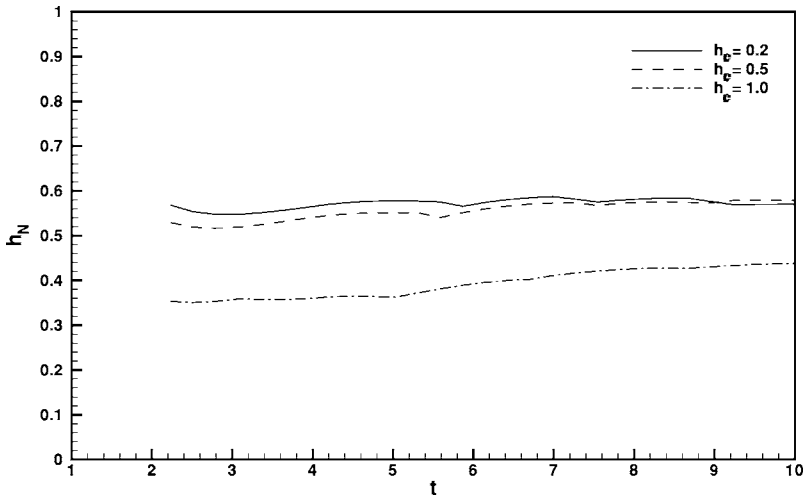

FIG. 4. The front height h_N as a function of time for gravity currents with S=0.2, Re=4000 and h_c=1, 0.5, and 0.2, respectively.

Downloaded 13 Jan 2009 to 130.95.144.214. Redistribution subject to AIP license or copyright; see http://pof.aip.org/pof/copyright.jsp

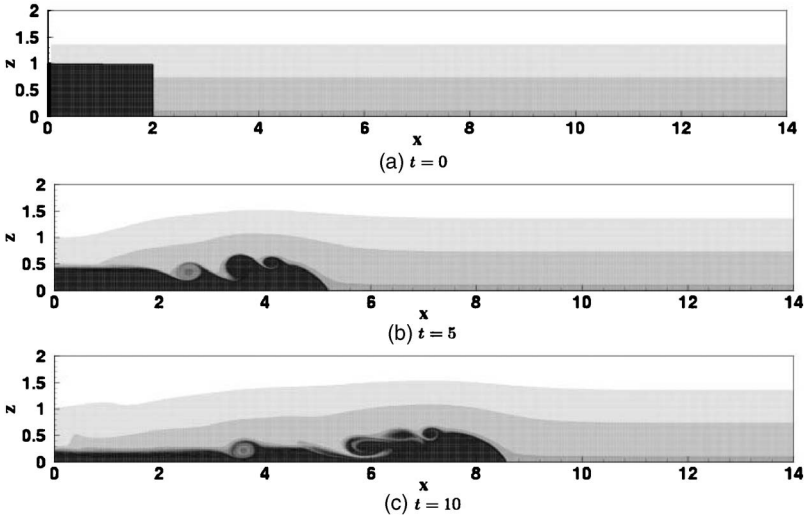

FIG. 5. Gravity current for stratification $S=0.2$ and initial lock height ratio $h_c=0.5$. Only a few weak vortices emerge behind the head of the current, whereas most of the trailing interface is stable.

strong vortices and intense mixing, cf. the discussions in Refs. 13, 11, 14, and 15. A straightforward measure of the front height can be obtained as the first local maximum of $h_l(x)$ coming from the right. However, due to the presence of the Kelvin-Helmholtz vortices, the front height thus obtained oscillates strongly with time. In order to obtain a more representative value of the front height that can be employed for the purpose of comparing with the theoretical analysis of Ref. 7, we hence evaluate the front height h_N by averaging the height of the first maximum over a sliding time interval of 1.5 units. Figure 4 indicates that h_N remains nearly constant after the initial adjustment phase. A more detailed discussion of this and other possible measures of the front height can be found in Ref. 12. For times beyond those shown in the figure, we expect that the bore reflected from the left wall will eventually catch up with the front and alter its shape. However, this interaction is beyond the scope of the current investigation.

2. Partial lock release

The flows for initial fractional depths of $h_c=0.5$ and 0.2 are shown in Figs. 5 and 6, respectively. For these deep water currents, the mixing layer behind the gravity current head is subjected to weaker shear, so that a much less pronounced Kelvin-Helmholtz instability is observed, although vortices can still be seen. The head has a more distinct shape and is more readily identifiable as compared to the full lock release case.

Figure 3 demonstrates that, just as the full release current, the partial lock release gravity currents also reach a constant velocity phase once they have gone through the initial adjustment phase. This quasisteady front velocity increases for lower values of h_c. For comparison with the theoretical predictions by Ref. 7, we employ the quasisteady front velocity at time $t=10$, along with the average value of the head height in the time interval $8\leq t\leq 10$, cf. Fig. 4.

B. Comparison with the theoretical predictions of Ungarish (Ref. 7)

Ungarish[7] adapts Long's model for stratified flow over topography[8–10] in order to obtain velocity and density profiles for a gravity current propagating into a stratified ambient. In this section we compare the computational results described above with the theoretical predictions by Ungarish.[7] In this context, it is to be kept in mind that the theoretical predictions apply to the region behind the head of the gravity current, where the streamlines are approximately horizontal. This results in some uncertainty when selecting the most suitable location for comparing with the theory, since the current height varies somewhat along the length of the current, in addition to undergoing slight temporal fluctuations. For a given stratification parameter S, head height $a=h_N h_c$ (head height scaled with channel depth), dimensionless front velocity U_H, and Froude number Fr_h, Ungarish[7] predicts a density profile of

$$\rho_l(z)=\begin{cases}1, & 0\leq zh_c\leq a,\\ r_b-zh_c(r_b-r_o)+(r_b-r_o)\dfrac{a}{\sin\gamma}\sin\left[\dfrac{\gamma}{1-a}(1-zh_c)\right], & a\leq zh_c\leq 1,\end{cases} \tag{10}$$

and a velocity profile, in the reference frame moving with gravity current front velocity U_H, of

Downloaded 13 Jan 2009 to 130.95.144.214. Redistribution subject to AIP license or copyright; see http://pof.aip.org/pof/copyright.jsp

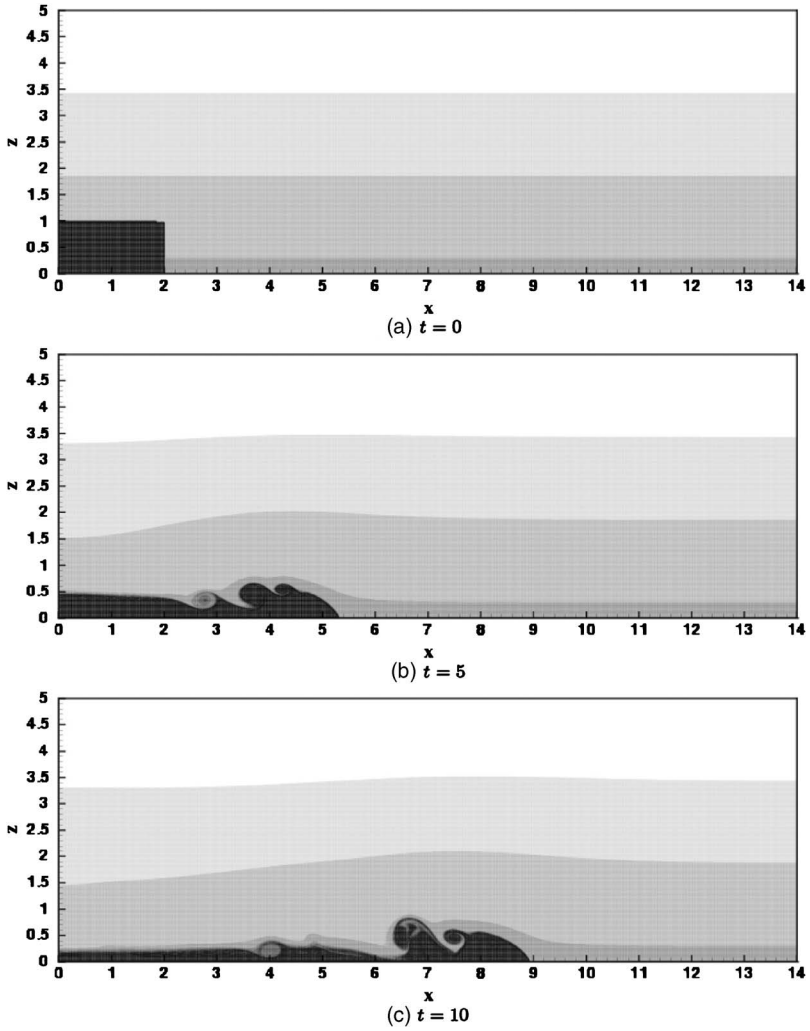

FIG. 6. Gravity current for stratification $S=0.2$ and initial lock height $h_c=0.2$. A raised current head can easily be identified, followed by a stable interface.

$$u_l(z)=\begin{cases}0, & 0\le zh_c\le a,\\ U_H\left(1+\dfrac{a}{1-a}\dfrac{\gamma}{\sin\gamma}\cos\left[\dfrac{\gamma}{1-a}(1-zh_c)\right]\right), & a\le zh_c\le 1,\end{cases} \tag{11}$$

where

$$\gamma=(1-a)\left(\frac{S}{a}\right)^{1/2}\frac{1}{\mathrm{Fr}_h}. \tag{12}$$

Figures 7 and 8 compare these theoretical predictions to the simulation results. The location at which the comparison is carried out needs to be chosen carefully. As we saw, for full lock releases the interface behind the current head is characterized by intense mixing, which in turn is caused by strong Kelvin-Helmholtz vortices. The presence of these vortices prevents the formation of a region with horizontal streamlines behind the current head, so that, strictly speaking, the assumptions made in the analysis by Ungarish[7] are not satisfied. However, we know that for a full lock release the time-averaged current height behind the head is nearly identical to the height of the head itself. In other words, the head is not raised above the trailing sections of the current.[13] Hence, the short region on top of the current head that is nearly horizontal and not yet subject to vortex shedding is suitable for a comparison with the theory. For the location one unit behind the tip of the current, which is not necessarily the location of the maximum current height, Fig. 7 shows the comparison of the computational density data at $t=10$ with the theoretical prediction. The slope of the density profile in the upper stratified fluid is predicted quite accurately by the theory. The uniformity of the slope suggests that the velocity field in the ambient at this location is quite uniform, so that the density gradient is not significantly deformed. The convective and diffusive mixing between the current fluid and the stratified ambient, which is not accounted for in the theory, leads to a smoothing of the interface between the two. Note that for the partial lock releases the location of this smoothed interface agrees more closely with the theoretical

Downloaded 13 Jan 2009 to 130.95.144.214. Redistribution subject to AIP license or copyright; see http://pof.aip.org/pof/copyright.jsp

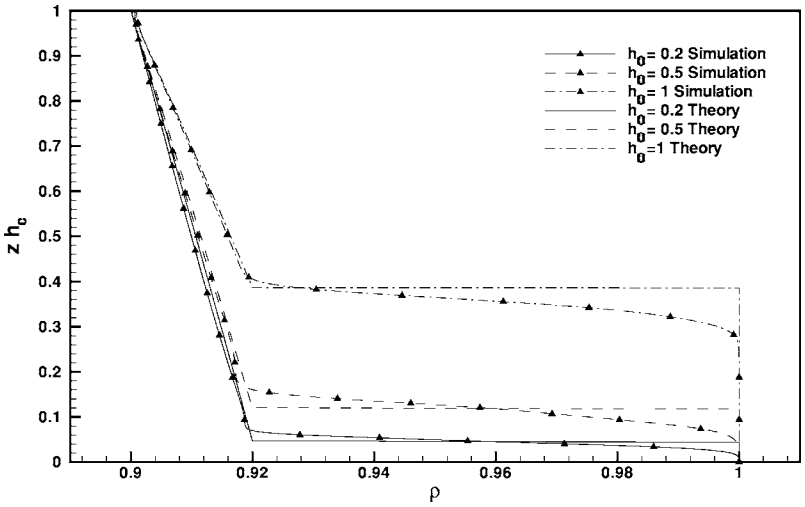

FIG. 7. Comparison of density profiles: Symbols indicate simulation results, while lines without symbols represent theoretical predictions by Ungarish (Ref. 7). Here the channel heights have been scaled such that they equal one for all three cases. Due to mixing of the current and ambient fluids, the jump in the theoretical density profiles is smoothed out in the simulations. However, the density profile in the stratified ambient is reproduced with good accuracy.

value than for the full lock release. This suggests that the theory works particularly well for shallow currents.

Figure 8 presents corresponding data for the velocity profile in the reference frame moving with the tip of the current. For the shallower currents we find that the fluid right above the current undergoes a significant acceleration. Note that the velocity profile within the current does not approach zero at the wall, as the fluid slightly behind the tip, and close to the wall, can move faster or more slowly than the tip itself. This result is well known from both computational investigations[13] and recent experimental measurements of intrusions.[16] Typically, for a full depth release the fluid near the wall moves faster than the head, while for a partial release the fluid in the trailing sections of the current moves more slowly than the head. Hence a positive or negative velocity in the reference frame moving with the tip can result. As the theory by Ungarish[7] considers the fluid in the current to be stagnant, it does not account for this effect. When comparing the streamwise velocity in the stratified ambient, we find that the qualitative shape is accurately predicted by the theory, although some moderate quantitative differences exist.

For the partial lock release cases of $h_c=0.5$ and 0.2, respectively, choosing a suitable location for comparing with the theory is much less critical, as large sections of the flow behind the head of the gravity current have a nearly horizontal interface. We choose $x=4.6$ and $x=5.0$ as the respective comparison locations. The results are shown in Figs. 7 and 8, along with the full lock release case. The comparison is similarly accurate as for the full lock case, indicating that the theoretical analysis applies equally well across the entire range of h_c values.

C. Effect of stratification on front velocity

Ungarish[7] employs Eqs. (10) and (11) to satisfy the force balance between far upstream and downstream of the gravity current head. After some algebra the following relationship between the Froude number Fr_h, the stratification parameter S and the fractional head depth a (ratio of height of the head to height of the ambient) is obtained

$$1-a+a(2-a)\gamma\cot\gamma+(a\gamma\cot\gamma)^2+\gamma^2\frac{a}{1-a}\left[(2-a)\left(1-\frac{1}{S}\right)-\frac{1}{3}a^2\right]=0, \tag{13}$$

with γ defined as above. For weak stratification (small S,γ), Ungarish[7] shows that the solution to Eq. (13) is given by

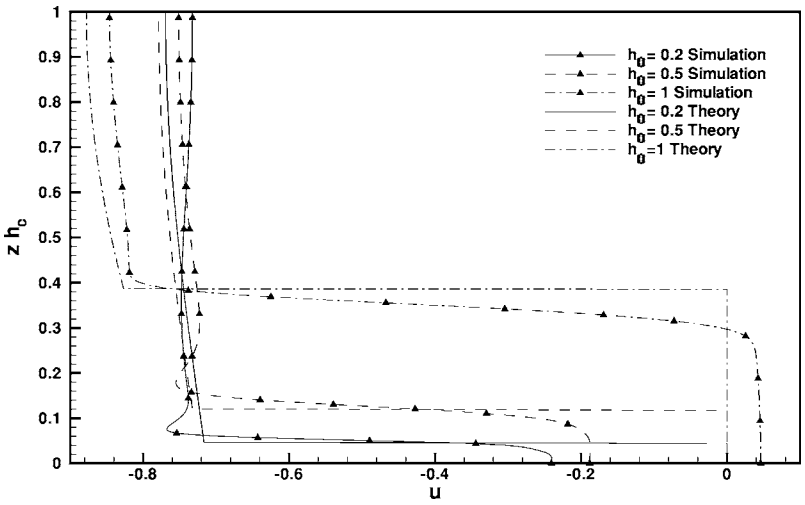

FIG. 8. Comparison of velocity profiles: Symbols indicate simulation results, while lines without symbols represent theoretical predictions by Ungarish (Ref. 7). The channel heights have been scaled such that they equal one for all three cases. The velocity of the ambient is predicted to a good degree of accuracy by the theory. Inside the current, there are substantial deviations from the theory, as the fluid behind the tip can move faster or more slowly than the tip itself. In contrast, the theory assumes that the current fluid stagnates, in the frame moving with the tip.

Downloaded 13 Jan 2009 to 130.95.144.214. Redistribution subject to AIP license or copyright; see http://pof.aip.org/pof/copyright.jsp

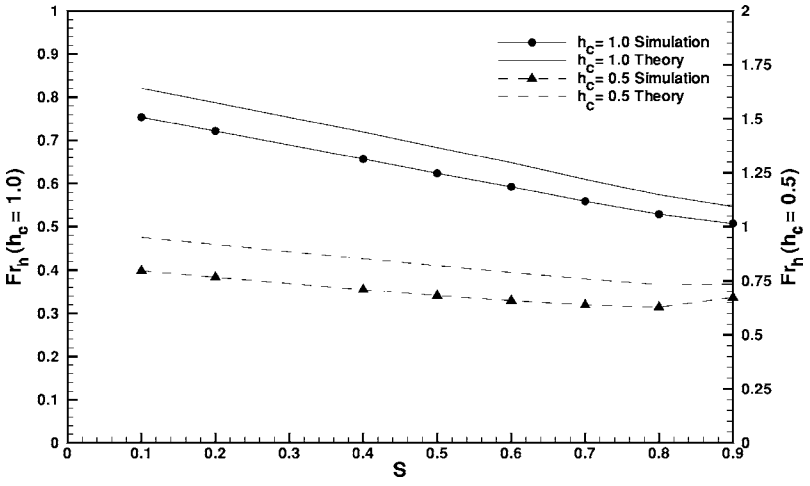

FIG. 9. The Froude number Fr_h of the gravity current as a function of the stratification parameter S for initial fractional depths of $h_c=1$ and 0.5, respectively. Solid line: theoretical prediction by Ungarish (Ref. 7); dashed line: simulation results. While the computational Froude number is somewhat smaller than the theoretical value, its dependence on S is in excellent agreement with the theory even for large values of S.

$$\mathrm{Fr}_h = \left[\frac{(2-a)(1-a)}{(1+a)}\left(1-\frac{2}{3}S\right)\right]^{1/2} = \mathrm{Fr}_B(a)\left(1-\frac{2}{3}S\right)^{1/2}, \tag{14}$$

where $\mathrm{Fr}_B(a)$ is the Benjamin solution for a gravity current propagating into an unstratified ambient.[2] Hence, for weakly stratified ambients the Froude number varies with S as $(1-2/3S)^{1/2}$. For strong stratification, multiple roots of Eq. (13) exist. This parameter regime will be discussed further in Sec. III D.

Figure 9 shows the comparison between the theoretically predicted and numerically obtained front velocities for $h_c=1$ and 0.5. In line with Ungarish's theoretical analysis, the current height is taken one unit length behind the current tip, where the streamlines are approximately horizontal. We observe that the computational results track the theoretical curve, although they lie somewhat below it. With regard to this comparison, one should keep in mind the uncertainties discussed above in selecting a region with a horizontal interface. Furthermore, the theory is inviscid, and based on the Boussinesq assumption.

We note in passing that various Froude number formulas have been suggested (for the $S=0$ case) that result in better agreement with experimental observations than Benjamin's result. These approaches lack the rigor of Benjamin's solution and contain adjustable constants. A known example is the semiempirical formula of Ref. 17. In a recent investigation of intrusions into nonstratified ambients, Nokes *et al.*[16] obtain the Froude number from a boundary element solution of the inviscid analysis of the local flow field near the current head. Interestingly, their values agree closely with the present observations in the limit of vanishing stratification, i.e., $S\to 0$. These comparisons are, however, outside the scope of the present study.

Figure 10 shows the corresponding comparison for $h_c=0.2$. At this value of the lock height, multiple solutions to Eq. (13) exist. The first solution, given by Eq. (14), is shown as a solid line without symbols. Additional solutions are denoted as second and third solutions, respectively, in the order in which they appear with increasing S. The dashed line with the triangle symbols indicates the numerically obtained front velocities. Good qualitative and reasonable quantitative agreement between the computational results and the first theoretical solution is observed for $S<0.5$. For $S>0.5$, however, we notice significant differences as the numerically computed front velocity decreases much more rapidly with increasing S than predicted by the first theoretical solution.

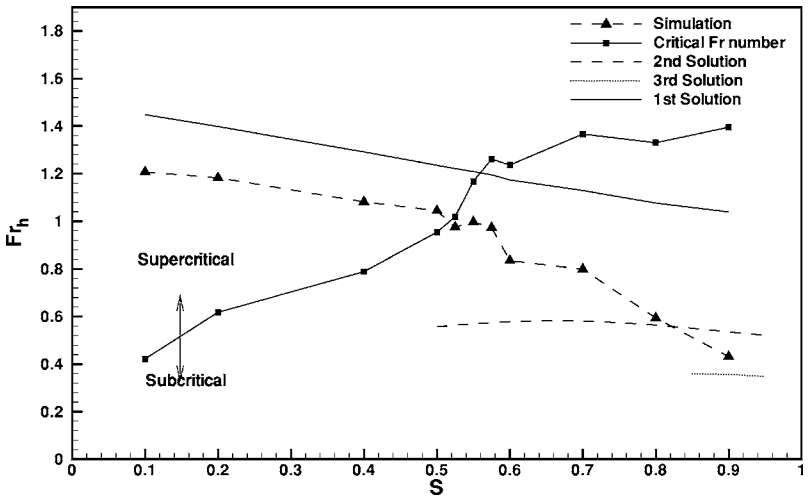

FIG. 10. The Froude number Fr_h of the gravity current as a function of the stratification parameter S, for an initial lock height of $h_c=0.2$. For this value of h_c and nonsmall S, multiple theoretical solutions exist. We observe good agreement between the first theoretical solution and the corresponding simulation results as long as the current moves faster than the fastest internal wave ($S<0.5$). If the current moves more slowly than the fastest internal waves ($S>0.5$), its front velocity agrees more closely with the second or third theoretical solution.

Downloaded 13 Jan 2009 to 130.95.144.214. Redistribution subject to AIP license or copyright; see http://pof.aip.org/pof/copyright.jsp

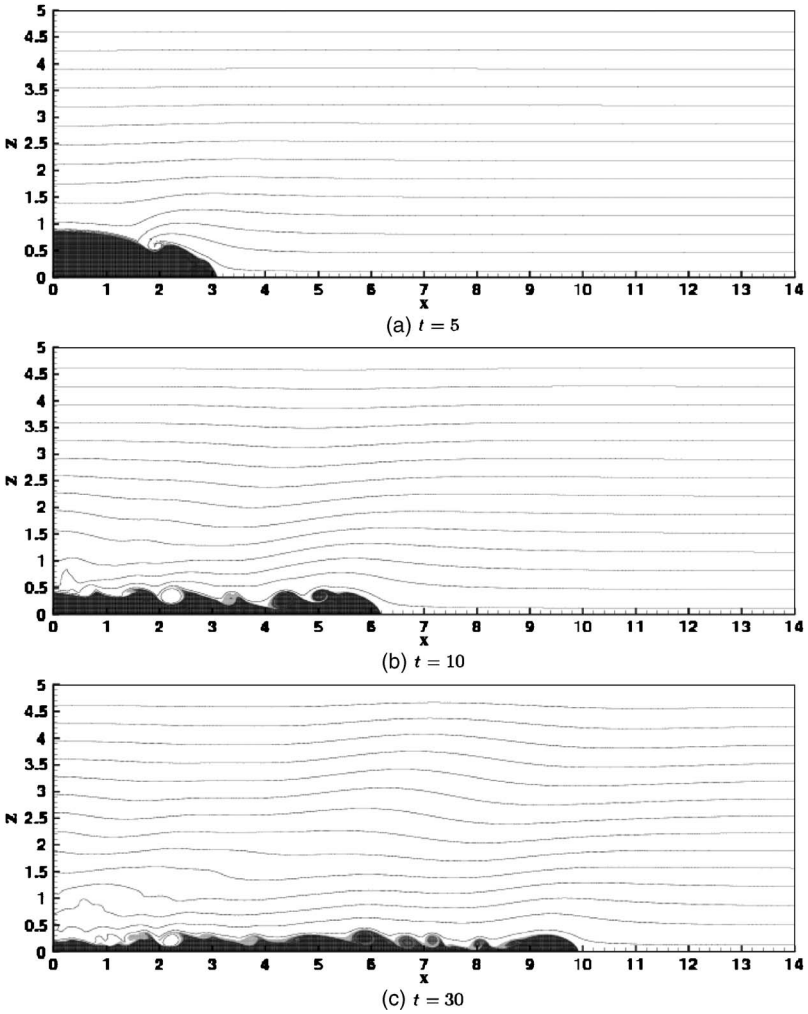

FIG. 11. Gravity current for $h_c=0.2$ and a strong background stratification of $S=0.9$. The concentration contours in the ambient suggest the existence of an internal wave, in contrast to the weak stratification case $S=0.2$ shown in Fig. 6.

For $S=0.8$ the numerical result is close to the second theoretical solution, while for $S=0.9$ it approaches the third theoretical solution.

The solid line with the square symbols represents the critical Froude number $\mathrm{Fr}_{\mathrm{cr}}$

$$\mathrm{Fr}_{\mathrm{cr}} = \frac{1}{\pi}\sqrt{\frac{S}{a}}, \tag{15}$$

which is defined as the value of Fr_h obtained for a current whose front velocity is equal to the speed of the fastest internal wave in the upstream ambient. A larger/smaller Fr_h corresponds to a super/subcritical current. We observe that for $S<0.5$ the current moves faster than the fastest internal wave, and its front velocity is predicted well by the first solution to Eq. (14). On the other hand, for $S>0.5$, the current moves more slowly than the fastest internal wave, and its front velocity is no longer predicted by Eq. (14). This observation is in agreement with Ungarish[7] and will be discussed in more detail in the next section.

D. Front velocity in the regime of multiple solutions

We will now explore in more detail the strong stratification regime, in which multiple solutions exist. Toward this end, we conduct a simulation for $h_c=0.2$ and $S=0.9$. Figure 11 displays the resulting density contours, which should be compared with the corresponding flow for $S=0.2$ shown in Fig. 6. The $S=0.9$ current has a noticeably smaller front height as compared to the $S=0.2$ flow. Furthermore, the density contours in the ambient suggest the presence of an internal wave, in contrast to the $S=0.2$ case. However, the observed upstream perturbation is very small. This confirms the assumption of the theory that even for subcritical currents the upstream conditions are well approximated by the original unperturbed linear density profile.

Figure 12 shows the dependence of the quasisteady front height h_N in the slumping phase (scaled with the height of the lock H_c) on the stratification and fractional depth. For a larger fractional depth and stronger stratification a smaller h_N is obtained. This is consistent with the energy-dissipation predictions of Ungarish.[7] Note, however, that the variation of h_N with S is very small for the full lock release. In particular, for the full-depth $h_c=1$ case the theory (see Fig. 6 in their paper) indicates that currents with $h_N=0.4$ have a small but acceptable head loss for $S<0.85$, while currents with $h_N=0.5$ display a negative (unacceptable) head loss for $S>0.2$. The numerically simulated h_N values are close to 0.4

Downloaded 13 Jan 2009 to 130.95.144.214. Redistribution subject to AIP license or copyright; see http://pof.aip.org/pof/copyright.jsp

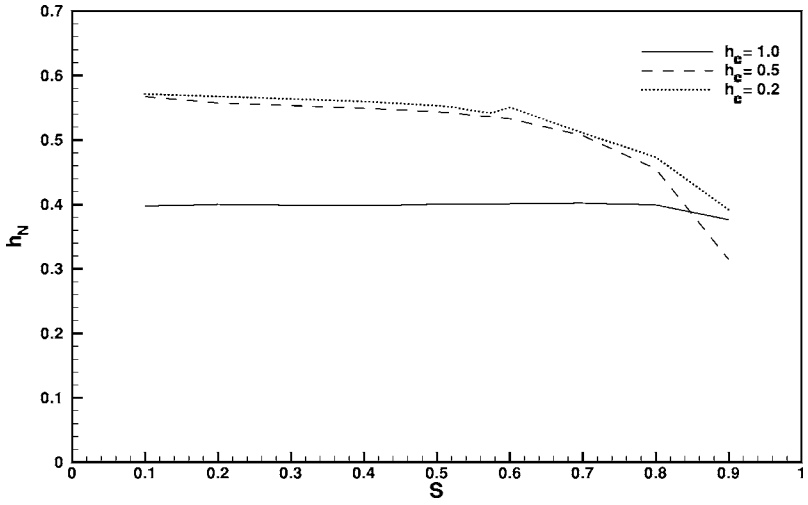

FIG. 12. Gravity current front height h_N as a function of stratification parameter S, for lock heights $h_c=0.2$, 0.5, and 1. For $h_c=1$ the front height is almost constant, while it decreases substantially at large S for $h_c=0.2$ and 0.5. This shows the selection of the slower solutions at large S and small a.

for $S<0.8$, then decrease slightly with S. We consider this agreement to be reasonable, on account of the possible contribution of viscosity to dissipation.

Upon release of the lock fluid, both the gravity current height and its front velocity vary with time before reaching a steady value, thus giving rise to an initially time-dependent Froude number. In order to explore this temporal evolution, Fig. 13 shows the front fractional depth $a=h_N h_c$ vs γ/π. The theory predicts that the domain of stable solutions for which Long's model is valid is below and to the left of the solid line. The shape of this domain has distinct regions separated from each other. Figure 13 provides a visual guide to the time evolution of the gravity current with respect to the domain of all valid physical solutions. Note that most of the symbols of a simulation tend to be clustered near one location in Fig. 13. The points away from this cluster represent the early time evolution, before the steady state Froude number is reached. The dotted line represents the critical propagation line; points above and to the right of this line represent subcritical propagation. Figure 13 indicates that stronger stratification generally tends to render the current subcritical, in agreement with Fig. 10. We note that all the numerical results are inside the domain of validity predicted by the theory, for both the transient phase and the quasisteady slumping phase of propagation. This provides strong support to the theoretical framework. An interesting novel observation is that the current preserves its mode of propagation with respect to the leading wave; all the points of a trajectory of a given current are either on the sub- or supercritical domain. Moreover, the data of the current with $h_c=0.2$ and $S=0.5$ (the squares) indicate a critical velocity of propagation (within a small deviation).

IV. CONCLUSION

The above detailed numerical simulations of gravity currents in stratified ambients demonstrate the power as well as the limitations of the theoretical analysis by Ungarish.[7] The functional dependence of the front velocity on the stratification parameter was found to agree with the theory for weak stratification, although the numerically obtained front velocities were somewhat smaller than the predicted values. These discrepancies are likely due to uncertainties in determining the height of the current. Furthermore, the theory is inviscid, while the simulations account for viscous effects.

Simulations for deeply submerged currents in strongly stratified ambients deviate from the fastest analytical solution, but fall within the range of the slower solutions found

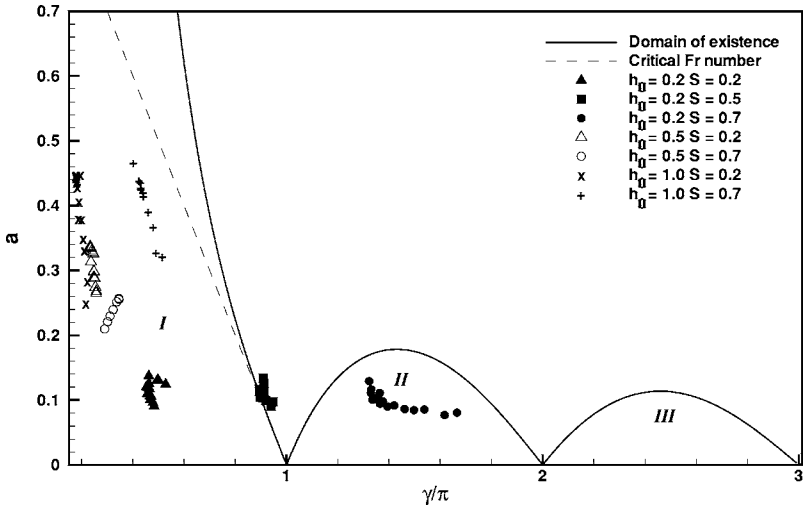

FIG. 13. The front fractional depth $a=h_N h_c$ vs γ/π, see (12). The figure shows that stronger stratification tends to render the current subcritical. The regions below and to the solid line are the domain of valid and stable flows according to the theoretical analysis by Ungarish (Ref. 7).

Downloaded 13 Jan 2009 to 130.95.144.214. Redistribution subject to AIP license or copyright; see http://pof.aip.org/pof/copyright.jsp

by Ungarish.[7] This observation supports the theoretical prediction that a time dependent flow will select the first attainable solution as the front velocity. The computational results indicate that the front velocity of the current released from rest is pushed toward the slower solutions by the action of internal waves that are generated by the current. Overall, the theory seems to provide the correct insights concerning the effect of the stratification. The quantitative deviations can be attributed to viscosity, non-Boussinesq, instability and wave effects, along with uncertainties related to selecting the most suitable location for the comparison. The discrepancies are similar to those obtained between Benjamin's results and nonstratified currents,[13] which is encouraging. We must keep in mind that the lock-release problem simulated in this work is able to cover only a limited region of the solution domain revealed by the ideal gravity current considered by Ungarish; in particular, a current released from rest can attain only one of the multiple results which are possible according to the theory. This leaves the realization of other solutions an open problem for further research.

ACKNOWLEDGMENTS

The authors acknowledge financial support by the National Science Foundation, and by BHP Billiton Petroleum.

[1] J. E. Simpson, *Gravity Currents in the Environment and the Laboratory* (Cambridge University Press, Cambridge, 1997).
[2] T. B. Benjamin, "Gravity currents and related phenomena," J. Fluid Mech. **31**, 209 (1968).
[3] J. Wu, "Mixed region collapse with internal wave generation in a density-stratified medium," J. Fluid Mech. **35**, 531 (1969).
[4] A. H. Schooley and B. A. Hughes, "An experimental and theoretical study of internal waves generated by collapse of a two-dimensional mixed region in a density gradient," J. Fluid Mech. **51**, 159 (1972).
[5] R. Amen and T. Maxworthy, "The gravitational collapse of a mixed region into a linearly stratified fluid," J. Fluid Mech. **96**, 65 (1980).
[6] T. Maxworthy, J. Leilich, J. E. Simpson, and E. Meiburg, "The propagation of gravity currents into a linearly stratified fluid," J. Fluid Mech. **453**, 371 (2002).
[7] M. Ungarish, "On gravity currents in a linearly stratified ambient: A generalization of Benjamin's steady-state propagation results," J. Fluid Mech. **548**, 49 (2006).
[8] R. R. Long, "Some aspects of the flow of stratified fluids. I. A theoretical investigation," Tellus **5**, 42 (1953).
[9] R. R. Long, "Some aspects of the flow of stratified fluids. III. Continuous density gradients," Tellus **7**, 341 (1955).
[10] P. G. Baines, *Topographic Effects in Stratified Flows* (Cambridge University Press, Cambridge, 1995).
[11] V. K. Birman, J. E. Martin, and E. Meiburg, "The non-Boussinesq lock-exchange problem. Part 2. High resolution simulations," J. Fluid Mech. **537**, 125 (2005).
[12] V. K. Birman, B. A. Battandier, E. Meiburg, and P. F. Linden, "Lock exchange flows in sloping channels," J. Fluid Mech. **577**, 53 (2007).
[13] C. Härtel, E. Meiburg, and F. Necker, "Analysis and direct numerical simulation of the flow at a gravity-current head. Part 1. Flow topology and front speed for slip and no-slip boundaries," J. Fluid Mech. **418**, 189 (2000).
[14] F. Necker, C. Härtel, L. Kleiser, and E. Meiburg, "High-resolution simulations of particle-driven gravity currents," Int. J. Multiphase Flow **28**, 279 (2002).
[15] F. Necker, C. Härtel, L. Kleiser, and E. Meiburg, "Mixing and dissipation in particle-driven gravity currents," J. Fluid Mech. **545**, 339 (2005).
[16] R. Nokes, M. Davidson, and C. Stepien, "A front condition for intrusive gravity currents," Proceedings of the 6th International Symposium on Stratified Flows (ISSF), edited by G. N. Ivey, The University of Western Australia, Perth, Australia, p. 434, 2006.
[17] H. E. Huppert and J. Simpson, "The slumping of gravity currents," J. Fluid Mech. **99**, 785 (1980).

Downloaded 13 Jan 2009 to 130.95.144.214. Redistribution subject to AIP license or copyright; see http://pof.aip.org/pof/copyright.jsp